

**Investigation of Electron Transport in Nanostructured
Semiconductor Heterojunctions by Using Dye-Sensitized Solid-
State Solar Cells**

by

Pitigala Kankanamage Don Duleepa Padmal Pitigala

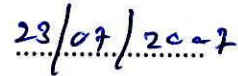
**Thesis submitted to the University of Sri Jayawardanapura for the
award of the Degree of Master of Philosophy in Physics on 2006**

DECLARATION

The work described in this thesis was carried out by me under the supervision of Prof. K Tennakone and Prof. D. A. Tantrigoda and a report on thesis has not been submitted in whole or in part of any university or any other institution for another Degree/Diploma.

A handwritten signature in blue ink, appearing to be 'D. A. Tantrigoda', written over a horizontal dotted line.

Signature of the candidate

A handwritten date '23/07/2027' in blue ink, written over a horizontal dotted line.

Date

I/We certify that the above statement made by the candidate is true and that this thesis is suitable for submission to the for the purpose of evaluation



(Signature)

23/07/2007

(Date)

Prof. K. Tennakone
Institute of Fundamental Studies,
Hantana Road,
Kandy, Sri Lanka.



(Signature)

25.07.2007

(Date)

Prof. D. A. Tantrigoda
Department of Physics,
University of Sri Jayawardanapura,
Nugegoda, Sri Lanka.



DEDICATION

TO

MY FATHER

MY MOTHER

AND

MY WIFE

CONTENTS

DECLARATION	
DEDICATION	
CONTENTS	i
LIST OF FIGURES & TABLES	vi
ACNOWLEDGEMENT	xv
ABBREVIATIONS	xvii
ABSTRACT	xix
CHAPTER 1	1-34
Introduction	1
1.1 Electron behavior in a crystal structure	1
1.1.1 Formation of covalent bonds	2
1.1.2 Formation of metallic bonds	2
1.1.3 Formation of energy bands in a crystal	3
1.2 Conductors semiconductors and nonconductors	4
1.3 Charge carriers in a semiconductors	5
1.4 Fermi-Dirac distribution function	9
1.4.1 Fermi Energy (W_F)	9
1.5 Degeneration of semiconductors	11
1.6 Junctions in a solids	12
1.6.1 Metal-metal junction	13
1.6.2 Metal-semiconductor junctions	14
1.6.3 Semiconductor-semiconductor junctions (p-n junctions)	17

1.7	Crystallinity in semiconductors	18
1.8	Semiconductor-light interaction	19
1.9	Photovoltaic cells	20
1.9.1	Metal-Schottky junction solar cells	21
1.9.2	Semiconductor-electrolyte junction solar cells.	21
1.10	Dye sensitized solar cells	23
1.10.1	Electron transport in DS Solid-State Solar Cell	23
1.10.2	Properties of n-TiO ₂	26
1.10.3	p-type semiconductors.	27
1.11	Theories equations related to solar cell devises.	28
1.11.1	Basic equations of device physics	29
1.11.2	Application of basic equations to homojunction solar sells.	30
1.11.3	Alternation of the device physics derivations for Dye sensitized systems (heterojunctions)	31
CHAPTER 2		35-52
Experimental and Characterization Methodology		35
2.1	Methodology	35
2.1.1	Preparation of conducting glass to deposition nanocrystalline TiO ₂ films	35
2.1.2	Preparation of TiO ₂ colloid for compact TiO ₂ Films	36
2.1.3	Preparation of CuI powder and CuSCN powder	36
2.1.3.1	Preparation of CuI powder	36

2.1.3.2	Preparation of CuSCN powder	37
2.1.4	CuSCN and CuI deposition technique	37
2.1.4.1	Deposition of CuSCN Films	37
2.1.4.2	Deposition of CuI Films	37
2.1.5	Dyes and Dye Solutions	38
2.1.6	Coating a monolayer of dye on the semiconductor surface	38
2.2	Fabrication of Dye sensitized solid state solar cell	39
2.3	Measurements and calculations	40
2.3.1	IV characteristics	41
2.3.2	Photocurrent action spectra and IPCE	45
2.3.3	Fluorescence	46
2.3.4	Mott-Schottky Plot	47
2.3.5	Dark IV plots (Rectification cuves)	48
CHAPTER 3		53-75
Electron transport in heterojunctions with two dyes		53
3.1	Introduction	53
3.2	Experimental	55
3.3	Results and Discussion	58
3.4	Conclusion	74
CHAPTER 4		76-94
Electron transport in a dye-semiconductor multilayered - semiconductor nanostructures		76

4.1	Introduction	76
4.2	Experimental	78
4.3	Results and Discussion	80
4.4	Conclusion	93
CHAPTER 5		95-108
Electron conduction in a nanostructure based on extremely thin - absorbat layer of polythiocyanogen.		95
5.1	Introduction	95
5.2	Experimental	96
5.3	Results and Discussion	98
5.4	Conclusion	108
CHAPTER 6		109-120
Strategy to enhancing the electron transport properties of CuSCN		109
6.1	Introduction	109
6.2	Experimental	110
6.3	Results and Discussion	112
6.4	Conclusion	120
CHAPTER 7		121-123
The addressable arias in future		121

REFERENCES

124-131

APPENDICES 1

132-134

LIST OF FIGURES and TABLES

	<i>Figure</i>	<i>Page No</i>
Figure 1.1	Plot of inter atomic energy vs atomic spacing. W_0 -bonding energy and r_0 is the separation of two atoms.	1
Figure 1.2	Illustration of energy band formation with the increment of number of atoms	3
Figure 1.3	Illustration of Energy bands in a metal, semiconductor and an insulator.	4
Figure 1.4	Illustration of the electron-hole mobility (intrinsic conduction) in a semiconductor (a) in a crystal lattice structure (b) in energy band structure.	6
Figure 1.5	Illustration of the Si lattice and energy band diagram doped with (a) Group III (Boron) and (b) Group V (Phosphorus) Atoms.	8
Figure 1.6	Fermi-Dirac function at absolute zero temperature ($T=0K$) and at higher temperatures ($T>0K$).	10
Figure 1.7	Energy diagrams of Degenerated p-type and n-type semiconductor.	11
Figure 1.8	Energy band diagrams of two metals (a) before and (b) after contact with each other	13
Figure 1.9	Band diagram of n-type semiconductor-metal junction where (a) $\Phi_m < \Phi_s$ and (b) $\Phi_m > \Phi_s$.	15
Figure 1.10	Band diagram of p-type semiconductor-metal junction where	

(a) $\Phi_m > \Phi_s$ and (b) $\Phi_m < \Phi_s$.	16
Figure 1.11 Energy band diagram of a p-n junction.	18
Figure 1.12 A schematic diagram of a photo electrochemical solar cell (PEC).	22
Figure 1.13 An energy band diagram of the DSS Solar Cell.	25
Figure 1.14 Illustration of recombination paths in a dye sensitized Solar Cell. (a) Recombination of CB electron with hole in the VB (b) Recombination pf CB electron with dye cation	25
Figure 2.1 Schematic diagram illustrating the cross section of a dye sensitized photovoltaic cell of heterostructure configuration of n-type semiconductor / Dye / p-type semiconductor.	40
Figure 2.2. (a) Illustration of schematic diagram of the IV setup and (b) A diagram of a Basic IV setup	42
Figure 2.3 illustration of a typical IV curve with maximum power point marked on it.	43
Figure 2.4 Figure illustrating the angel of the sun for different AM conditions.	44
Figure 2.5 Action spectra and IPCE curve of a DSSC with a double dye system.	45
Figure 2.6 Illustration of excitation of electrons by absorbing photons and emmision of radiation due to diexcitation.	47
Figure 2.7 Mott-Schotky plot of (a) p-type semiconductor (b) n-type semiconductor	48
Figure 2.8 Illustration of band bending when the semiconductor	

	electrode is biased different voltages	50
Figure 2.9	Illustration of a Mott-Schottky setup	51
Figure 2.10	Dark I-V (rectification) characteristic curve	52
Figure 3.1	Schematic diagrams showing the construction of the cell TiO ₂ /D ₁ -D ₂ /CuSCN.	57
Figure 3.2	(I) I-V characteristics of (a) TiO ₂ /MV/CuSCN (b) TiO ₂ /TA- MV/CuSCN and (II) Photocurrent action spectra of (a) TiO ₂ /MV/CuSCN (b) TiO ₂ /TA-MV/CuSCN	59
Figure 3.3	Schematic diagrams illustrating possible configurations of double-dye solid-state solar cells, (I) homogenously mixed thick layer two dyes (II) a monolayer consisting of two non- interacting dye molecules coupled to n and p-type semiconductors (III) dye layer consisting of two electronically coupled dye molecules bonded on opposites sides to n and p-type semiconductors (circles indicate two types of dye molecules).	62
Figure 3.4	Schematic energy level diagram indicating the relative positions of conduction bands (CB) and valence bands (VB) of TiO ₂ and CuSCN and ground and excited levels of the D ₁ and D ₂ (a) charge transfer on excitation of D ₁ (b) charge transfer on excitation of D ₂ .	64
Figure 3.5	Photocurrent action spectrum of (a) TiO ₂ /MC-MV/CuSCN (b)TiO ₂ /MC/CuSCN (c) TiO ₂ /MV/CuSCN	68

- Figure 3.6 Photocurrent action spectrum of the cells (a) $\text{TiO}_2/\text{BR}/\text{CuSCN}$ 69
 (b) $\text{TiO}_2/\text{BR-IR786}/\text{CuSCN}$.
- Figure 3.7 Structural unit in the double dye system n-type semiconductor/
 $\text{D}_1\text{-D}_2/\text{p-type semiconductor}$ (B = bridge connecting the 71
 chromophores).
- Figure 3.8 Schematic diagram indicating possible intermediate stages of
 charge injection to n-type (boxes on right) and p- type (boxes
 on left) semiconductors when dye molecules D_1 (circles on
 left) and D_2 (circles on right) are excited (a) excitation of D_1
 followed by electron transfer between two dye molecules and
 subsequent electron injection of n-type material and holes to
 the p-type material. (Similar steps occur when D_2 gets
 excited) (b) Possible electron transfer schemes when carrier
 injection to the semiconductor is the initial step. 72
- Figure 3.9 Rectification curves of the cells with dyes (a) MV (b) MC (c)
 MC-MV 73
- Figure 4.1 Diagram illustrating the construction of the photovoltaic cell
 of heterostructure configuration (a) $\text{TiO}_2/\text{D}_1/\text{CuSCN}/\text{D}_2/$
 CuSCN (b) $\text{TiO}_2/\text{D}_1/\text{CuSCN}/\text{D}_2/\text{CuSCN}/\text{D}_3/\text{CuSCN}$. 79
- Figure 4.2 I-V characteristics of the cells, [a] $\text{TiO}_2/\text{D}_1/\text{CuSCN}$ [b]
 $\text{TiO}_2/\text{CuSCN}/\text{D}_2/\text{CuSCN}$ [c] $\text{TiO}_2/\text{D}_1/\text{CuSCNS}/\text{D}_2/\text{CuSCNS}$,
 where $\text{D}_1 = \text{Fast Green}$, $\text{D}_2 = \text{Acridine Yellow}$. 82
- Figure 4.3 Photocurrent action spectra of the cells [a] $\text{TiO}_2/\text{D}_1/\text{CuSCN}$
 [b] $\text{TiO}_2/\text{CuSCN}/\text{D}_2/\text{CuSCN}$ [c] $\text{TiO}_2/\text{D}_1/\text{CuSCN}/\text{D}_2/\text{CuCNS}$ 83

- Figure 4.4 Energy level diagram showing the band structure in $\text{TiO}_2/\text{CuSCN}/\text{D}/\text{CuSCN}$, ground (S^0) and excited (S^*) levels of the dye D and the modes of electron-hole transfer when the dye is photo-excited. 85
- Figure 4.5 Energy level diagram showing the band structure in $\text{TiO}_2/\text{D}_1/\text{CuSCN}/\text{D}_2/\text{CuSCN}$, the positions of the ground (S^0_1, S^0_2) and excited (S^*_1, S^*_2) levels of the two dyes (D_1, D_2). The dyes D_1 (FG) and D_2 (AY) anchored to TiO_2 and CuSCN respectively 86
- Figure 4.6 (i) Absorption spectrum of aqueous solutions of (a) $\text{D}_3 =$ Acridine Yellow (b) $\text{D}_2 =$ Rhodamine 6G (c) $\text{D}_1 =$ Fast Green; (ii) Photocurrent action spectrum of the cell $\text{TiO}_2/\text{D}_1/\text{CuSCN}/\text{D}_2/\text{CuSCN}/\text{D}_3/ \text{CuSCN}$. 89
- Figure 4.7 An energy level diagram showing the conduction and valence band edges of TiO_2 and CuSCN and the ground (S^0_1, S^0_2, S^0_3) and excited (S^*_1, S^*_2, S^*_3) levels of the dyes $\text{D}_1, \text{D}_2, \text{D}_3$. ($\text{D}_1 =$ Fast Green, $\text{D}_2 =$ Rhodamine 6G, $\text{D}_3 =$ Acridine Yellow). 90
- Figure 4.8 I-V characteristics of the 3-dye cell $\text{TiO}_2 / \text{D}_1 / \text{CuSCN}/\text{D}_2 / \text{CuSCN}/\text{D}_3 / \text{p-CuSCN}$. 92
- Figure 5.1 Schematic diagram of the Construction of the photovoltaic cell with $(\text{SCN})_n$ layer. 98
- Figure 5.2 FT-IR spectrum of the polythiocyanogen scraped off from a film deposited on conducting tin oxide glass (T=Transmittance). 99

Figure 5.3	The Mott-Schottky plot for a film of polythiocyanogen deposited on conducting glass. Measurement frequency: (a)1.5kHz, (b) 1.0 kHz.	101
Figure 5.4	Absorption spectrum of a polythiocyanogen film and photocurrent action spectrum of the cell $\text{TiO}_2/[\text{SCN}]_n/\text{CuI}$	102
Figure 5.5.1	SEM picture of bare conducting tin oxide glass surface	103
Figure 5.5.2	SEM picture of polythiocyanogen deposited on conducting tin oxide glass surface.	103
Figure 5.5.3	SEM picture of bare nanocrystalline TiO_2 film	104
Figure 5.5.4	SEM picture of polythiocyanogen deposited on a nanocrystalline film of TiO_2 .	104
Figure 5.6	I-V characteristics of the cell $\text{TiO}_2/[\text{SCN}]_n/\text{CuI}$ measured at 1000 Wm^{-2} , 1.5AM illumination.	105
Figure 5.7	Schematic energy level diagram of conduction and valance band positions of TiO_2 , $[\text{SCN}]_n$ and CuI .	106
Figure 5.8	Dark IV (rectification curve) for the cell $\text{TiO}_2/[\text{SCN}]_n/\text{CuI}$	107
Figure 6.1	Graph of Time variation of the sheet resistance of the CuSCN films when they are inserted into a N_2 atmosphere containing (a) Cl_2 (b) Br_2 (c) I_2	113
Figure 6.2	Graph of Change in sheet resistance of the CuSCN films doped with (a) I_2 (b) Br_2 (c) Cl_2 when kept in a N_2 atmosphere	115
Figure 6.3	Fluorescence spectrum of (a) CuSCN film on glass (b) CuSCN film on glass exposed to Cl_2 . Inset: Energy level representation of the $(\text{SCN})_2$ impurity level in CuSCN .	116

Figure 6.4 I-V characteristic of the cell TiO₂/Ru-dye/ CuSCN (a) before exposure to (SCN)₂ solution in CCl₄. (b) after exposure to (SCN)₂ solution in CCl₄. 118

Figure 6.5 Mott-Schottky plots of a CuSCN film on CTO glass (a) before exposure to (SCN)₂ solution (b) after exposure to (SCN)₂ solution. 119

Schemes

Page No

Scheme 3.1 Anchoring of the sodium salt of trihydroxybenzoic acid to TiO₂ and attachment of methyl violet cation by replacement of Na⁺ 59

Scheme 3.2 The mode of anchoring of mercurochrome to TiO₂ and attachment of methyl violet cation by replacement of Na⁺. 65

Scheme 3.3 The mode of anchoring of bromopyrogallol red to TiO₂ and attachment of IR 786 cation by replacement of Na⁺. 66

Tables

Page No

Table 3.1 Short-circuit photocurrent (I_{sc}), open-circuit voltage (V_{oc}), efficiency (η), fill-factor (FF) and peak (620 nm) incident photon to photocurrent conversion efficiency (IPCE) of TiO₂/MV/CuSCN and TiO₂/TA-MV/CuSCN 60

Table 3.2	Incident photon to photocurrent conversion efficiencies (IPCEs) of the cells (1) TiO ₂ / MC-MV/ CuSCN (2) TiO ₂ / MC/ CuSCN (3) TiO ₂ / MV/ CuSCN at peak absorption wavelengths of the two dyes.	67
Table 3.3	Incident photon to photocurrent conversion efficiencies (IPCEs) of the cells (1) TiO ₂ / BR-IR786/ CuSCN (2) TiO ₂ / BR/ CuSCN (3) TiO ₂ / IR786/ CuSCN at peak absorption wavelengths of the two dyes.	68
Table 3.4	Open-Circuit Voltage (V_{oc}), Short-Circuit Photocurrent (I_{sc}), Fill factor (FF) and Energy conversion efficiency (η) of the cells (1) TiO ₂ / MC- MV/ CuSCN (2) TiO ₂ / MC/ CuSCN (3) TiO ₂ / MV/ CuSCN (4) TiO ₂ / BR- IR786/ CuSCN (5) TiO ₂ / BR/ CuSCN (6) TiO ₂ / IR786/ CuSCN.	70
Table 4.1	Short circuit photocurrent (I_{sc}), open-circuit voltage (V_{oc}), Fill Factor (FF) and efficiency (η) of photovoltaic cells of different configurations	81
Table 4.2	Incident photon to photocurrent conversion efficiencies (IPCEs) of different heterostructure configurations at the peak absorption wavelengths of the two dyes D ₁ (FG, 650nm) and D ₂ (AY, 470 nm).	83
Table 4.3	Short-circuit photocurrents (I_{sc}), open-circuit voltages (V_{oc}) and efficiencies of dye-sensitized solid-state photovoltaic cells of different configurations (D ₁ = Fast Green, D ₂ = Rhodamine 6G, D ₃ = Acridine Yellow).	93

Table 6.1 The short-circuit photocurrent (I_{sc}), open-circuit voltage (V_{oc}), efficiency (η), and fill factor (FF) of the cells TiO_2 /Dye/CuSCN before and after SCN doping of CuSCN film. 118

ACKNOWLEDGMENTS

I wish express my most sincere thanks and gratitude to my supervisor, Prof. K. Tennakone; the project leader of the Condensed Matter Physics Project and the Director of Institute of Fundamental Studies, Kandy, for his guidance, valuable advice, encouragement and emotional support given to me throughout my research period.

I wish to convey my appreciation and thanks to my supervisor Prof. D. A. Tantrigoda, Professor of Physics, Department of Physics, University of Sri Jayawardanapura, for the guidance and advice given to me during the period of the study.

I wish to convey my grateful thanks to Dr. V. P. S Perera, Visiting Scientist, Institute of Fundamental Studies, Kandy and Senior Lecturer, Open University of Sri Lanka, Nawala, and he is also my colleague in early period of my work; for his guidance and encouragement given to me. Also I wish to thank Dr. Perera especially for proof reading and valuable advice.

I wish to express my appreciations to Dr. P. M. Sirimanna, Project Leader of the Nano Science Project, Institute of Fundamental Studies, Kandy, for his help and kind advise given to me in the latter period. My grateful thanks are also due to Dr. G. R. A. Kumara, and Dr. I. R. M. Kottegoda for helping me to obtain the SEM pictures and FTIR measurements of my samples.

I am also very much grateful to my colleagues Ms. M. K. I. Senevirathna and Mr. E. V. A. Premalal, Research Assistants of the Condensed Matter Physics project, Institute of Fundamental Studies, Kandy, for their continues support paid on me in writing the thesis. Also I wish to convey my thanks to former research assistants Mr. P. V. V. Jayaweera and Ms. K. M. P. Bandaranayaka for the support given to me in the initial period of my work.

I would like to convey my thanks Mr. W.G. Jayasekara, the laboratory technician of the condensed matter physics project for the help given to me in varies ways in completion of this thesis. Also I wish to thank all the other research and nonresearch staff members of the I. F. S. for there intentional or unintentional support given to me in completion of my work.

ABBREVIATIONS

AY	- Acradin Yellow
AM	-Atmospheric mass
BR	-Bromopyrogallol Red Dye
CB	-Conduction Band
Cu	-Copper
DS	-Dye Sensitized
DSPEC	-Dye sensitized photo electro chemical solar cell
DSSSC	-Dye sensitized solid state cell
D	-Diffusion coefficient / Dye molecule
D_i	-Ground state or ground state energy level dye molecules of the i^{th} dye layer
D_i^*	-Excited state or excited state energy level dye molecules of the i^{th} dye layer.
e	-electron
FF	-Fill Factor
FG	-Fast Green
Ge	-Germanium
h	-hole
i.e.	-That is
K.E	-Kinetic energy
CuI	-Copper Iodide.
CuSCN	-Copper thiocyanate

CuSCN	-Thick layer of p-type semiconductor Copper thiocyanate
<i>CuSCN</i>	-Thin layer of p-type semiconductor Copper thiocyanate
MC	-Mercurochrome dye
MV	-Methyl Violet dye
P.E	-Potential energy
S	-Sulphur
SC	-Solar Cell
SCE	-Standard Calomel Electrode
CSN ⁻	-thiosyanate ion
S ⁰	-Ground State Energy
S [*]	-Exited State Energy
Si	-Silicon
TiO ₂	-Titanium Dioxide
τ	-recombination time
VB	-Valence Band
W	-work
wt	-weight

Investigation of electron transport in nanostructured semiconductor heterojunctions by using dye-sensitized solid-state solar cells

Pitigala Kankanamage Don Duleepa Padmal Pitigala

ABSTRACT

In this study an attempt has been made to understand the electron transport phenomenon in nanostructure heterojunctions with a view to solve the problems related to recombination and the narrow spectral response of dye sensitized solid state solar cells.

It has been reported in literature that attempts to broaden the spectral response by using multiple dyes have resulting in decreasing photocurrent due to concentration quenching and sub monolayer chelation. However it was revealed that if the two dyes are bonding ionically together with each other, it gives better spectral response and a higher photocurrent. Two such double dye systems are discussed in this work. The Mercurochrome-Methyl violet system shows a spectral response from about 500nm to 650nm, with a 4.6 mAcm^{-2} photocurrent density. The Bromopyrogallol red-IR786 system shows a spectral response extended to infrared region in addition to the increase in the photocurrent. The rectification characteristic curves of these systems also show suppression of the recombination too.

It was also investigated the possibility of using dye-semiconductor multilayers for this purpose and found to yield reasonably acceptable results. It was found that the two dyes Fast green and Acridine yellow when used in the multistructure give an efficiency of 1.67% which is significantly higher than there individual efficiencies. The problem arises when the system extended to more than two dyes is also studied.

Application of a barrier to recombination too is an effective methodology to enhance the performance of a solar cell. The polymer polythiocyanogen is found highly stable and resistant to heat and chemical action. A barrier for recombination is constructed by depositing polythiocyanogen in the heterojunction to study the performance. The polymer polythiocyanogen also acts as the sensitizer of the solar cell.

Conductivity of the p-type semiconductor in the solid state dye sensitized solar cell is also important to its performance. Copper (I) thiocyanate is an important p-type semiconductor satisfying the high band-gap requirements of the above solar cells. However the conductivity of this material is not sufficiently high. The conductivity of solid CuSCN was altered by exposing it to halogen gases and SCN^- ions in CCl_4 . The latter method is found more suitable for doping of CuSCN films in the heterojunction of dye-sensitized solid-state solar cells. A photocurrent of 9.0 mAcm^{-2} was achieved by doping CuSCN with SCN^- ions and it is more than 300% increase in the photocurrent.